25th ABCM International Congress of Mechanical Engineering
October 20-25, 2019, Uberlândia, MG, Brazil

COBEM2019-0437
INFLUENCE OF SYNTHESIS PARAMETERS ON BARIUM TITANATE STRUCTURAL PROPERTIES OBTAINED BY MICROWAVE ASSISTED SOLVOTHERMAL METHOD

Amanda Pereira dos Santos da Costa
Yuri Vinicius Bruschi de Santana
Ana Paula de Moura
Universidade Tecnológica Federal do Paraná, Campus Cornélio Procópio, Paraná, Brasil.
amanda-1233@hotmail.com; yurisantana@utfpr.edu.br; apdemoura@gmail.com.

Abstract. *The aim of this work is to obtain barium titanate's powders synthesized by microwave assisted solvothermal method (MASM) and observe the effects of synthesis parameters on the structural properties. The studied parameters were: temperature, alkaline concentration of medium, acid washing and posterior calcination on half of the samples. The expected effects were that these establishments could produce dielectric active powders, and free from impurities, of this material with a grain size in the nanoscale. The main results were satisfactory concerning to the purity of the samples according to the DRX of the material. X-ray diffractions showed a cubic, and pseudo cubic phase accordingly to the used parameters.*

Keywords: *Barium titanate, solvothermal method, perovskite, characterization, morphology.*

1. INTRODUCTION

Barium titanate belongs to a large group of crystals named as perovskites, which its principal characteristic is the center atom is slightly dislocated, allowing the appearing of an instantaneous electric dipole, when presented on its tetragonal form below the Curie temperature, being possible the emergence of a high dielectric constant, which allows the increasing miniaturization of devices year after year. Also, its ferroelectricity and piezoelectricity permit it to be one of the most used ceramics in applications of multilayer capacitors, thermistors, piezoelectric device, microwave dielectric ceramics, or even in optical devices (Vijatović et al., 2008).

Many techniques are possible to produce barium titanate, such as conventional hydrothermal (Dutta et al., 1992), polymeric precursor (Vinothini, 2006), solid state reaction and oxalate precipitation (Simon-Seveyrat, 2007) and others. The microwave assisted hydrothermal/solvothermal method has some advantages in comparison to the conventional method in terms of rapid crystallization kinetics and energy efficiency, including the possibility of obtaining tetragonal particles directly from the synthesis (Sun, 2006).

Thinking about that, this work sought to obtain nano powders of barium titanate through MASM under relatively low temperature and time of synthesis, varying the alkaline concentration among 1M, 8M and 10M to pursue effects on morphology of grain sizes and formats. Also, acid washing was used to eliminate barium carbonate formed together with the main material. Ultimately, half of each sample was separated and put into calcination to produce the tetragonal phase of the material and compensate the limitations of low temperature of the synthesis.

2. MATERIALS AND METHODS

2.1 Obtaining the material

The MASM synthesis of barium titanate was performed in four stages:

a) Reagents preparation: at this stage, three different beckers containing 50 ml of an alkaline solution between potassium hydroxide and titanium (IV) isopropoxide previously dissolved in 30 ml of ethyl alcohol were put into constant stirring and heating (80°C) for 90 min to eliminate the entire alcohol. Parallel to this, three other beckers were used to dissolve barium chloride in 50 ml of distilled water. Passed those 90 min, both beckers were put together to complete a solution of 100 ml containing the base, acting as the medium of reaction, titanium (IV) isopropoxide and barium chloride. The samples are specified accordingly to their reagent's concentrations, duration of synthesis, temperature and concentration of the base on Table 1.

Table 1. Samples specifications concerning the used reagents, duration and temperature of synthesis, alkaline concentration, as well as which samples were calcinated.

sample	barium chloride (mol)	titanium (IV) isopropoxide (mol)	time	temperature (°C)	base concentration (mol/l)	calcinated
1	0.03	0.03	32 min	160	1M	No
2					8M	
3					10M	
1.1					1M	Yes
2.1					8M	
3.1					10M	
BT12h	0.03	0.03	12 h	160	1M	No

b) Synthesis: each of the samples was sealed into an autoclave, coupled with a microwave oven attached on a PID controller, schematized in Figure 1.

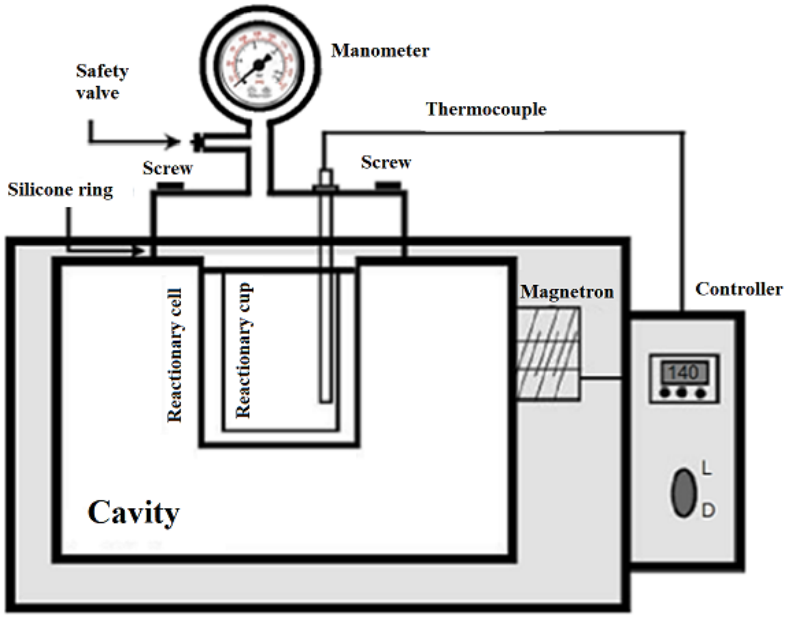

Figure 1. Scheme of the autoclave coupled to a microwave oven attached to the PID controller. Adapted from: Santana, 2013.

c) Washing and drying: after all samples were obtained, each one was separated into plastic recipients and taken to a centrifuge to be washed seven times with a solution of acetic acid (0.1 M) and other three times with distilled water. Lastly, they were placed in Petri dishes to dry on the heated plaque under 90°C for a few hours.
d) Calcination: the three samples, after dried, were split in half. This second half was put into an oven and calcinated for 4 hours under 900°C with the purpose of making grain growth and turn the cubic particles into tetragonal particles.

2.2 Characterization

The characterization of all samples was made by X-ray diffraction, using the diffractometer Xpert PRO MPD, brand PANanalytical, radiation Cu-Kα (λ=1.5406 Å), scan rate of 0.05°/s to a 2θ interval from 15° to 80°. Also, calculations about grain sizes were made using Scherrer's equation:

$$cs = k*\lambda / \beta*cos(\theta) \quad (1)$$

Where k = Scherrer's constant (0.9) for spherical crystallites with cubic symmetry; λ = X-ray wavelength; θ = angle of diffracted peak and β = full width at half maximum (FWHM).

Bragg's law was used to calculate interplanar distances and unit cell parameters. The value of n = 1 was considered for a first order diffraction as follows:

$$d = n*\lambda / 2*sin(\theta) \quad (2)$$

$$a = d_{[h, k, l]}*(h^2 + k^2 + l^2)^{1/2} \quad (3)$$

The peak broadening that happens in X-ray diffractions involving samples makes the observation of the tetragonal phase rather difficult, that's why an alternative verification of sample's tetragonality can be made through comparison of ratios between FWHM and peak height intensities of planes (111) and (200) accordingly to some references in literature (Hayashi et al., 2013 and Hakuta et al., 2005):

$$H_{(111)}/H_{(200)} > 1 \text{ (tetragonal)} \quad (4)$$

$$FWHM_{200}/FWHM_{111} > 1 \text{ (tetragonal)} \quad (5)$$

FTIR and SEM images were also used for characterization of samples.

3. RESULTS AND DISCUSSION

Concerning the purity of samples, X-ray patterns have showed a monophasic barium titanate on the first three samples, although, only two of the calcinated samples appeared to have a pure phase, the one synthesized under lower concentration of alkaline medium presented the formation of an impurity. Firstly, the X-ray diffractions for samples without calcinating are presented in Figure 2 and further characterizations in the following tables.

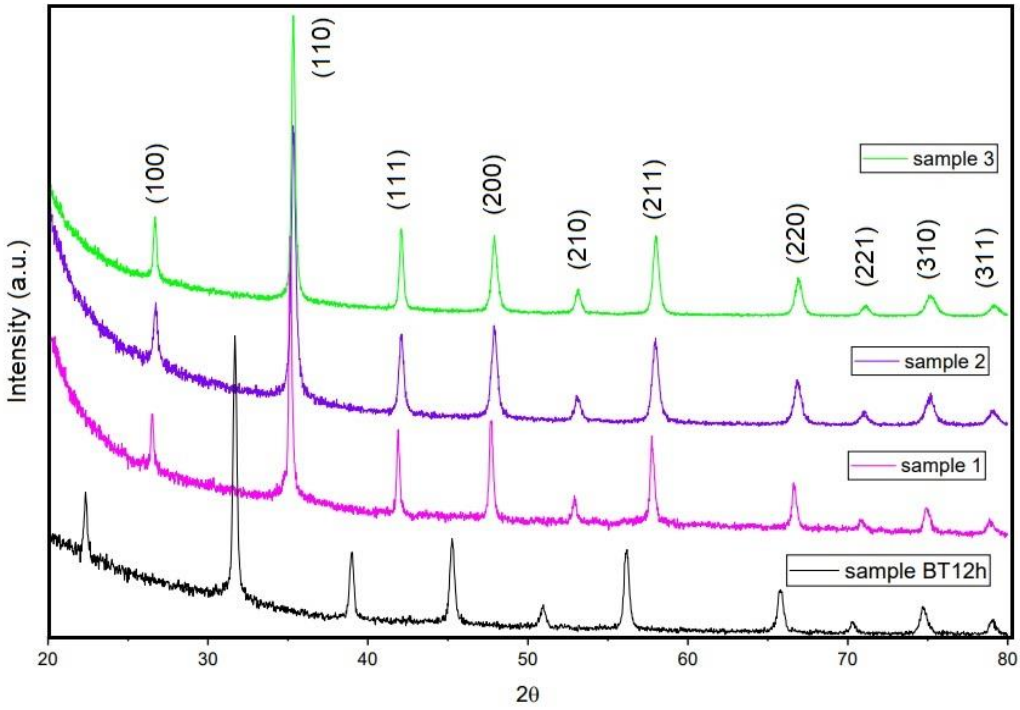

Figure 2. X-ray diffractions for samples obtained with variations on time of synthesis and alkaline concentration. Own authorship.

It can be seen that, the more alkaline the environment becomes, smaller the crystallite size gets, and, at 10M, tetragonal phase is achieved, due to higher intensity in the peak of plane (111) in comparison to plane's (200) intensity. The other samples, despite having slightly larger FWHM of their (200) planes in comparison to (111), this last one has lower intensity of peak, becoming uncertain the affirmation of the existence of the tetragonal phase.

In this case of synthesis at low temperature, the strength of pH is a more determinant variable than time to obtain the tetragonal phase, what appears to be a good thing, taking into account that higher durations of synthesis requires lot more energy, making the process impracticable.

Average crystallite sizes, estimated with equation 1, for the samples shown above are presented in Table 2.

Table 2. Average crystallite sizes for samples 1, 2, 3 and BT12h estimated with Scherrer's equation

sample	crystallite size (nm)	sample	crystallite size (nm)
1	38.43	3	23.21
2	30.05	BT12h	38.59

From Bragg's law, the average unit cell parameter for each of the samples presented above are set out in Table 3:

Table 3. Average values for unit cell parameters with its standard deviations.

sample	unit cell parameter (Å)	standard deviation	sample	unit cell parameter (Å)	standard deviation
1	4.03	0.00093	3	4.01	0.0035
2	4.01	0.0064	BT12h	4.01	0.0066

The biggest grain size belongs to sample 1, which also has the largest unit cell parameter. Perhaps, the lower concentration of pH influenced the grains to be coarser due to the best dilution of precursors as higher the environment's pH becomes (Özen et al., 2016).

The calcinated samples' X-ray diffractions are plotted in Figure 3 and their respective characterizations are showed in Tables 4 and 5.

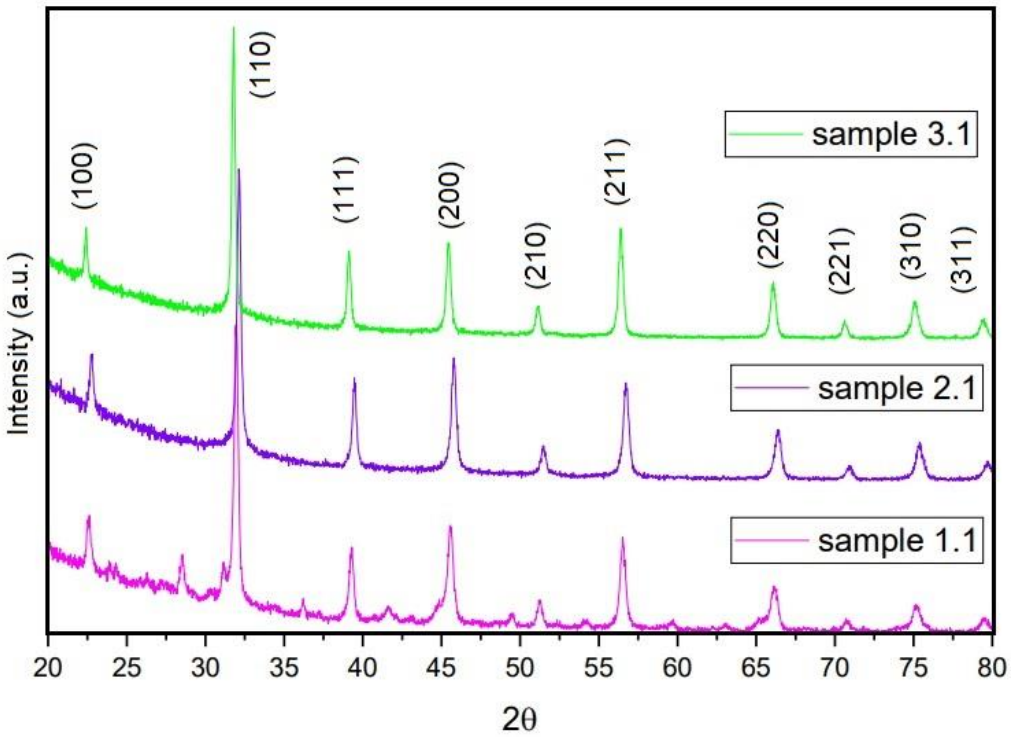

Figure 3. X-ray diffractions for samples obtained varying only alkaline concentration for precursors. Own authorship

Average crystallite sizes, estimated with equation 1, for the samples shown above are presented in Table 4:

Table 4. Average crystallite sizes for samples 1.1, 2.1 and 3.1 estimated with Scherrer's equation

sample	crystallite size (nm)
1.1	30.92
2.1	23.31
3.1	30.91

There was a reduction in crystallite size due to calcination for samples 1.1 and 2.1, although, for sample 3.1 there was an increase. The average unit cell parameter for each of the samples presented are set out in Table 5.

Table 5. Average values for unit cell parameters with its standard deviations

sample	unit cell parameter (Å)	standard deviation
1.1	3.98	0.013
2.1	3.97	0.012
3.1	3.99	0.0045

FTIR for the four samples shown is presented as follows.

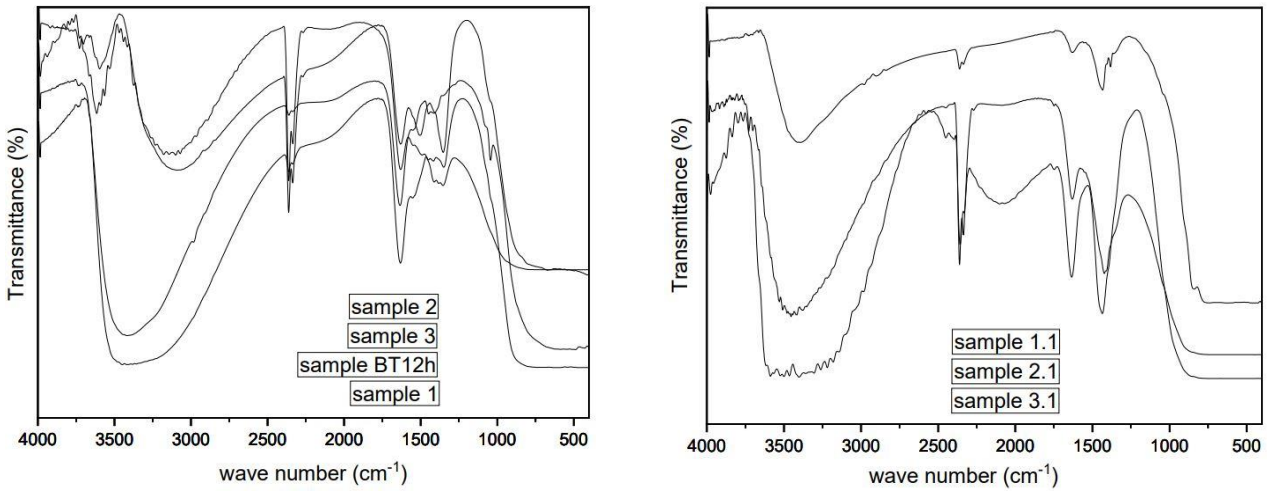

Figure 4. Infrared spectra for samples represented from bottom to top accordingly to the order of presented names.
Own authorship.

For the non-calcinated samples, the stretch that happens in 3205 cm^{-1} has been identified as the stretching mode of OH ions commonly presented in perovskites structures grown at low temperatures, because of the high mobility of hydrogen in perovskite materials. It is also possible to observe that, as long as the alkaline concentration increases, less intense becomes the peak around this wave number. Also, the broad band at 557 cm^{-1} is due to Ti-O vibrations in $BaTiO_3$ (Sengodan et al. 2012).

It can be seen that, calcinating the powders, for samples 2 and 3, the intensity of the OH stretching vibrations around 3430 cm^{-1} and 1425 cm^{-1} became stronger, while for sample 1, obtained at the lowest alkaline concentration, happened the reduction of the OH corresponding peak, indicating the reduction in the dipolar moment in the bonding.

SEM images for the non-calcinated samples are shown in sequence.

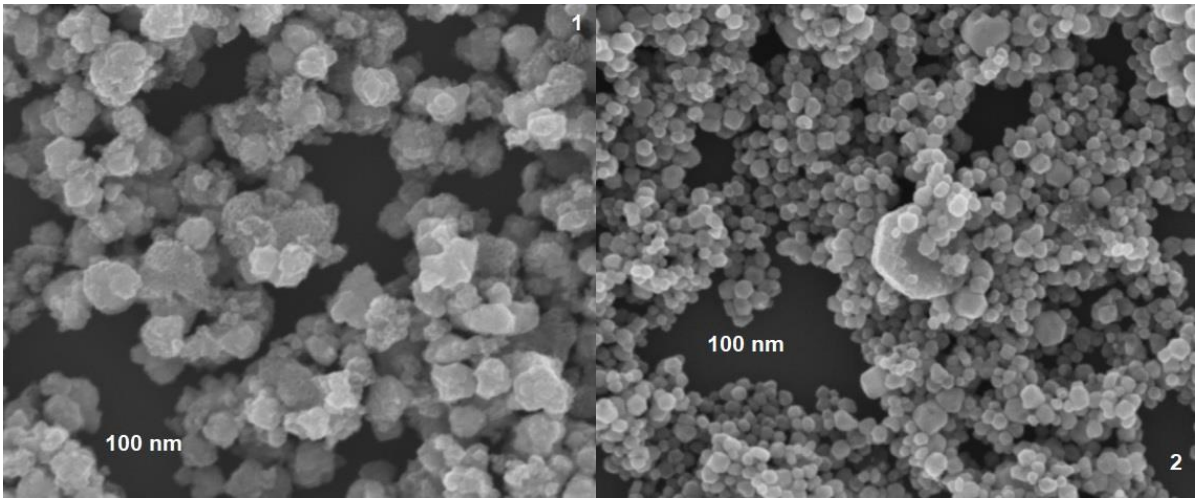

Figure 5. SEM images for samples 1 and 2.
Own authorship.

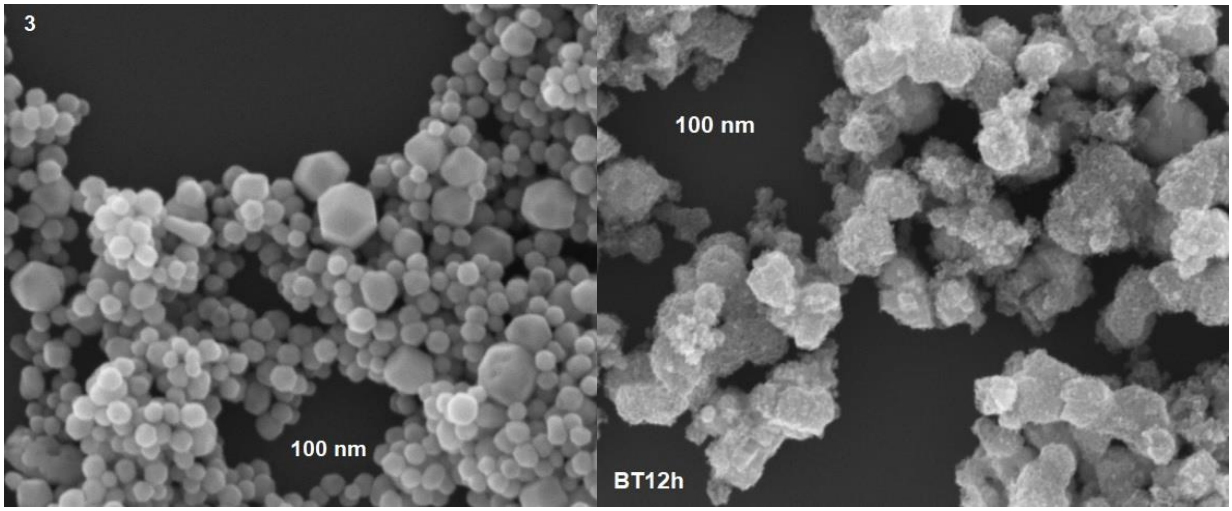

Figure 6. SEM images for samples 3 and BT12h.
Own authorship.

It is possible to observe that samples 1 and BT12h, synthesized at the same pH concentration, presented similar grain morphologies, although the second one was made at a much longer time. This indicates that, when alkaline concentration is low, time is not a decisive parameter in grain morphology. Their grains don't have a well-defined shape, but it is possible to verify a tendency to coalescence in the whole region observed in both samples.

Sample 2 already has well-defined spherical shapes, with some regions possessing a few bigger grains than the others and also a strong presence for coalescence.

Sample 3, synthesized at the highest alkaline concentration, possesses regions in which it is possible to observe some hexagonal shapes, but a larger quantity of crystallites still has spherical shapes.

SEM images for the calcinated samples are presented as follows.

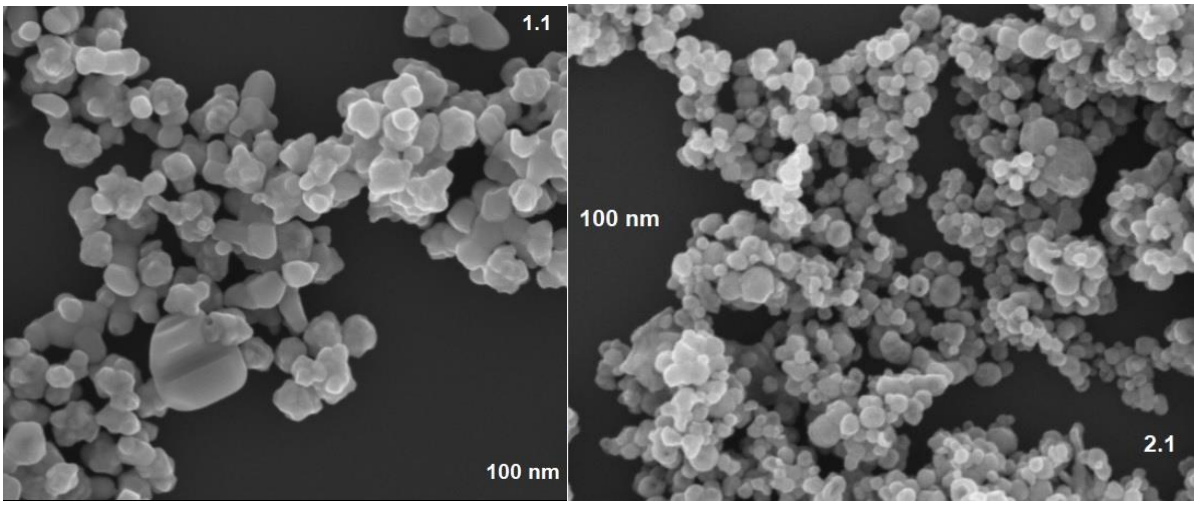

Figure 7. SEM images for the calcination of samples 1 and 2.
Own authorship.

In sample 1.1, synthesized at the lowest alkaline concentration among them, the formation of impurities occurred, which, according to some literature, may be the result of the reaction of barium titanate with barium carbonate, due to the presence of hot air (Zhang, 1996).

Comparing this with the other two, which presented pure phase of BT, it is assumed that higher base concentrations make it difficult to form impurities.

Cubic symmetry was formed in all three samples, including calcination of sample 9, which had previously reached its tetragonal shape.

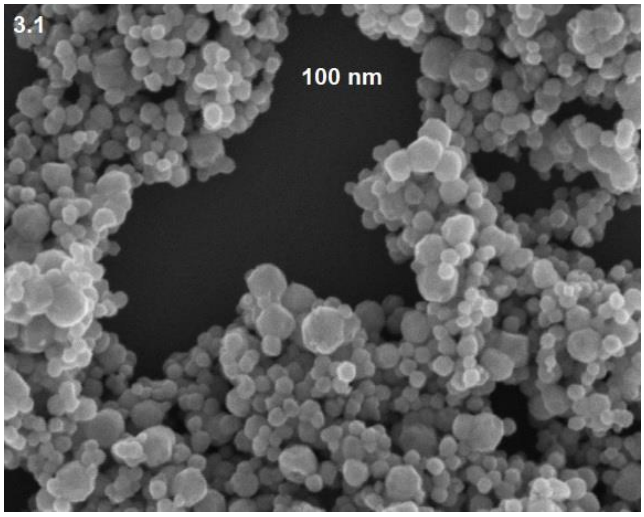

Figure 8. SEM image for calcination of sample 3.
Own authorship.

This last image proves the crystallite growth indicated in Table 4, where it is possible to see several regions occurring coalescence of grains to form a bigger one.

4. CONCLUSIONS

The microwave assisted solvothermal method, MASM, was successful in obtaining tetragonal and monophasic powders of barium titanate, $BaTiO_3$, at a temperature of 160°C and time of synthesis of 32 min, having the alkaline concentration of medium as a determinant to synthesize the material.

When synthesizing at a temperature lower than 170°C, pH is a more decisive variable than time in obtaining tetragonal phase.

Calcinating the samples at 900°C for 4h was not enough to transform the cubic phase into tetragonal, actually, it turned into cubic the sample that had already became tetragonal from the synthesis. In addition of this, for a material synthesized at lower pH, it occurred the appearance of an impurity, stating that higher concentrations of base are better for obtention of BT powders.

5. REFERENCES

Dutta, P. K.; Gregg, J. R.. Hydrothermal synthesis of tetragonal barium titanate (BaTiO3). Chemistry of Materials, [s.l.], v. 4, n. 4, p.843-846, jul. 1992. American Chemical Society (ACS). http://dx.doi.org/10.1021/cm00022a019.

Habib, A.; Haubner, R.; Stelzer, N.. Effect of temperature, time and particle size of Ti precursor on hydrothermal synthesis of barium titanate. Materials Science and Engineering: B, [s.l.], v. 152, n. 1-3, p.60-65, ago. 2008. Elsevier BV. http://dx.doi.org/10.1016/j.mseb.2008.06.018.

Hakuta, Y. et al. Effect of water density on polymorph of BaTiO3 nanoparticles synthesized under sub and supercritical water conditions. Materials Letters, [s.l.], v. 59, n. 11, p.1387-1390, maio 2005. Elsevier BV. http://dx.doi.org/10.1016/j.matlet.2004.11.063.

Hayashi, H. et al. In-situ Raman spectroscopy of BaTiO3 particles for tetragonal–cubic transformation. Journal Of Physics And Chemistry Of Solids**,** [s.l.], v. 74, n. 7, p.957-962, jul. 2013. Elsevier BV. http://dx.doi.org/10.1016/j.jpcs.2013.02.010.

Hoshina, T. et al. Composite structure and size effect of barium titanate nanoparticles. Applied Physics Letters, [s.l.], v. 93, n. 19, 10 nov. 2008. AIP Publishing. http://dx.doi.org/10.1063/1.3027067.

Özen, M. et al. Hydrothermal synthesis and formation mechanism of tetragonal barium titanate in a highly concentrated alkaline solution. Ceramics International, [s.l.], v. 42, n. 9, p.10967-10975, jul. 2016. Elsevier BV. http://dx.doi.org/10.1016/j.ceramint.2016.03.234.

Santana, Y. V. B. de. Estudo das propriedades ópticas e estruturais de nanocristrais de ZnS, obtidos pelo método solvotérmico aquecido por micro-ondas. 2013. 90 f. Tese (Doutorado em Ciências) – Departamento de Química, Universidade Federal de São Carlos, São Carlos, 2013.

Sengodan, R. et al. Synthesis and Characterization of BaTiO3 Nano particles by Organic Precursor Method. International Journal Of Modern Engineering Research. Coimbatore, p. 43-45. mar. 2012. Available at: <https://pdfs.semanticscholar.org/a853/cab610d62ae651af6a027777350ac9bfe7f0.pdf>. Access in: 19 jul. 2019.

Simon-Seveyrat, L. et al. Re-investigation of synthesis of BaTiO3 by conventional solid-state reaction and oxalate coprecipitation route for piezoelectric applications. Ceramics International, [s.l.], v. 33, n. 1, p.35-40, jan. 2007. Elsevier BV. http://dx.doi.org/10.1016/j.ceramint.2005.07.019.

Sun, W.; Li, J.. Microwave-hydrothermal synthesis of tetragonal barium titanate. Materials Letters, [s.l.], v. 60, n. 13-14, p.1599-1602, jun. 2006. Elsevier BV. http://dx.doi.org/10.1016/j.matlet.2005.11.078.

Suzuki, K.; Kijima, K.. Size driven phase transition of barium titanate nanoparticles prepared by plasma chemical vapor deposition. Journal Of Materials Science, [s.l.], v. 40, n. 5, p.1289-1292, mar. 2005. Springer Nature. http://dx.doi.org/10.1007/s10853-005-6954-9.

Vijatović, M.M.; Bobić, J.D.; Stojanović, B.D.. History and challenges of barium titanate: Part I. Science of Sintering, [s.l.], v. 40, n. 2, p.155-165, 2008. National Library of Serbia. http://dx.doi.org/10.2298/sos0802155v.

Vinothini, V.; Singh, P.; Balasubramanian, M.. Synthesis of barium titanate nanopowder using polymeric precursor method. Ceramics International, [s.l.], v. 32, n. 2, p.99-103, jan. 2006. Elsevier BV. Http://dx.doi.org/10.1016/j.ceramint.2004.12.012.

Zhang, H. et al. Kinetics and Mechanism of the Microwave Synthesis of Barium Titanate. Mrs Proceedings, [s.l.], v. 430, jan. 1996. Cambridge University Press (CUP). http://dx.doi.org/10.1557/proc-430-447.

6. RESPONSIBILITY NOTICE

The authors are the only responsible for the printed material included in this paper.